https://doi.org/10.5194/amt-2021-7
Preprint. Discussion started: 10 February 2021

Atmospheric Measurement Techniques Discussions

Evaluation of satellite retrievals of liquid clouds from the GOES-13 Imager and MODIS over the midlatitude North Atlantic during NAAMES campaign

David Painemal[1,2], Douglas Spangenberg[1,2], William L. Smith Jr. [2] , Patrick Minnis[1,2], Brian Cairns[3], Richard H. Moore[2], Ewan Crosbie[1,2], Claire Robinson[1,2], Kenneth L. Thornhill[1,2], Edward L. Winstead[1,2], and Luke Ziemba[2]

[1]Science Systems and Application Systems, Inc.
[2]NASA Langley Research Center
[3]NASA Goddard Institute for Space Studies
Correspondence to: David Painemal (david.painemal@nasa.gov)

Abstract. Satellite retrievals of cloud droplet effective radius (r_e) and optical depth (τ) from the Thirteenth Geostationary Operational Environmental Satellite (GOES-13), and the MOderate resolution Imaging Spectroradiometer (MODIS) onboard Aqua and Terra are evaluated with airborne data collected over the midlatitude boundary layer during the North Atlantic Aerosols and Marine Ecosystems Study (NAAMES). The airborne dataset comprises in-situ r_e from the Cloud Droplet Probe (CDP) and remotely sensed r_e and τ from the airborne Research Scanning Polarimeter (RSP). GOES-13 and MODIS (Aqua and Terra) r_e values are systematically greater than those from the CDP and RSP by at least 4.8 μm (GOES-13) and 1.7 μm (MODIS) despite relatively high linear correlations coefficients (r = 0.52 – 0.68). In contrast, the satellite τ underestimates its RSP counterpart by -3.0, with r = 0.76 – 077. Overall, MODIS yields better agreement with airborne data than GOES-13, with biases consistent with those reported for subtropical stratocumulus clouds. While the negative bias in satellite τ is mostly due to the retrievals having been collected in highly heterogeneous cloud scenes, the causes for the positive bias in satellite r_e, especially for GOES-13, are more complex. Although the high viewing zenith angle (~65˚) and coarser pixel resolution for GOES-13 could explain a r_e bias of at least 0.7 μm, the higher GOES-13 r_e bias relative to that from MODIS is likely rooted in other factors. In this regard, a near monotonic increase was also observed in GOES-13 r_e up to 1.0 μm with satellite scattering angle (Θ) over the angular range 116˚-165˚, that is, r_e increases toward the backscattering direction. Understanding the variations of r_e with Θ will require the combined use of theoretical computations along with inter-comparisons of satellite retrievals derived from sensors with dissimilar viewing geometry.

https://doi.org/10.5194/amt-2021-7
Preprint. Discussion started: 10 February 2021


Atmospheric Measurement Techniques Discussions

1. Introduction

Cloud properties estimated from satellite passive sensors have been crucial in advancing our knowledge of the role of clouds in the climate system and the Earth's energy budget (e.g. *Loeb et al.*, 2009; *Kato et al.*, 2011). The unprecedented global view from space has been facilitated by a constellation of more than a dozen satellites equipped with visible and infrared imagers suitable for the derivation of cloud properties. Among the various satellite sensors orbiting Earth, the MOderate resolution Imaging Spectroradiometer (MODIS) on Terra and Aqua is the most widely used in cloud and climate research due to its high radiometric performance and relatively high pixel resolution, and the ability to provide nearly global spatial coverage by combining the multiple daily satellite overpasses. Complementary to MODIS, a number of geostationary satellites with adequate sensor wavelengths for deriving cloud properties comparable to MODIS are currently applied by various remote sensing groups around the world to detect clouds and derive cloud phase, effective radius, optical depth, liquid/ice water path, and height (*Stubenrauch et al.*, 2013; *Roebeling et al.*, 2015). These geostationary cloud properties are receiving increased attention as their high temporal resolution allows for continuous monitoring of cloud systems, making the datasets ideal for numerous weather applications, including nowcasting and data assimilation (e.g., *Benjamin et al.* 2016; *Jones et al.* 2018).

Passive-based cloud algorithms typically rely on a visible channel for retrieving cloud optical depth and an absorbing near-infrared channel for estimating cloud effective radius (r_e), which, in turn, can be utilized for indirectly estimating liquid water path. Numerous studies have documented factors that can possibly bias the passive satellite cloud retrievals based on bi-spectral algorithms, including among others: sub-pixel variability, clear-sky contamination, solar and viewing angles effects, as well as three-dimensional radiative effects (e.g. *Marshak et al.* 2006; *Kato et al.* 2006, *Zhang et al.*, 2012). Despite these sources of uncertainty, comparisons between in-situ aircraft data and MODIS retrievals for marine stratocumulus clouds have shown excellent correlations for effective radius, optical depth, and liquid water path in the eastern Pacific and northeast Atlantic (*Painemal and Zuidema*, 2011; *Painemal et al.*, 2012; *Noble and Hudson*, 2015; *Zhang et al.*, 2018). In contrast, *Ahn et al.* (2018) found poor agreement between MODIS cloud effective radius and airborne cloud probe measurements over the Southern Ocean. Unfortunately, the limited number and complexity of the samples in *Ahn et al.* (2018) prevented further inferences, an issue that illustrates the challenges of evaluating satellite observations in middle and high latitudes.

In-situ and remotely sensed aircraft observations of cloud properties are key for evaluating cloud retrievals, however, sparse sampling and observational uncertainties hamper the satellite bias quantification. Optimal airborne measurements for assessing satellite observations should incorporate data redundancy, samples taken at different levels within the cloud, and use of observations within minutes of the satellite overpass time. Data redundancy helps minimize the misinterpretation of biases in satellite observations, whereas cloud vertical sampling allows for a more adequate comparison with satellite products, especially retrieved particle size, which is primarily contributed by a few optical depths from the cloud top (*Platnick*, 2000). Here we take advantage of aircraft measurements taken over the midlatitude North Atlantic during the North Atlantic Aerosols and Marine Ecosystems Study (NAAMES, *Behrenfeld et al.*, 2019), which employed a sampling strategy well suited for evaluating satellite observations. NAAMES deployed

https://doi.org/10.5194/amt-2021-7
Preprint. Discussion started: 10 February 2021


Atmospheric Measurement Techniques Discussions

the NASA C-130 aircraft to measure cloud and aerosol properties during three campaigns in November 2015, May 2016, and September 2017 over the approximate domain of 50˚W-35˚W, 38N-60˚N (Fig. 1).

Both NAAMES airborne in-situ and remotely sensed observations are used to evaluate satellite retrievals of liquid cloud effective radius and optical depth from the Thirteenth Geostationary Operational Environmental Satellite (GOES-13), and from the MODIS onboard Aqua and Terra. The cloud properties were derived using the algorithms developed for the Clouds and the Earth's Radiant Energy System (CERES). The NAAMES observational dataset comprises in-situ cloud observations collected by a Cloud Droplet Probe (CDP) and a Cloud Imaging Probe (CIP), and remotely sensed retrievals from the NASA Goddard Institute for Space Studies (GISS) airborne Research Scanning Polarimeter (RSP). A special emphasis is placed on the inter-satellite differences and the role of pixel resolution and viewing geometry in accounting for the observed discrepancies.

2. Dataset

2.1.Airborne observation

The NAAMES domain, aircraft tracks, and the mean Aqua-MODIS low cloud fraction (cloud tops < 3 km) are depicted in Fig. 1. The region features mean cloud fractions greater than 0.65, with the dominant presence of supercooled cloud tops during the cold months (*Hu et al.*, 2010), and corroborated by NAAMES RSP data. The C-130 flew approximately 60-100 min per mission between 09:00 LT to 15:00 LT, corresponding to a solar zenith angle ranging from 23˚ to 81˚ (mean solar zenith angle of 51˚). Cloud sampling was limited to boundary layer liquid clouds with a mean cloud top height of 1376 m±602 m (± standard deviation).

Cloud droplet size distributions were sampled in-situ with a CDP manufactured by Droplet Measurements Technologies (DMT, Inc., Boulder, CO). The CDP probe is a forward-scattering optical spectrometer that measures droplet sizes between 2 and 50 μm with bin widths of 1 μm and 2 μm for droplet diameters larger or smaller than 14 μm, respectively. A main source of uncertainty is the oversizing and undercounting of droplet concentrations higher than 400 cm^{-3} (*Lance* et al., 2010). This issue has a limited effect for NAAMES as the liquid cloud droplet number concentration remained below 250 cm^{-3} during the campaigns. Unfortunately, post-deployment evaluation at DMT revealed that the probe operated with a sampling area larger than the manufacturer specifications, yielding an overcounting of droplets for all the bins. This overcounting is thought to equally affect each bin, implying that the cloud effective radius is little affected by the sampling area problem. Considering the unresolved problem with the CDP probe, cloud effective radius is the only in-situ cloud observation used for quantitative assessments in this study. The error introduced by the larger instrument sample area in other quantities (water content, extinction coefficient, and cloud droplet number concentration) requires further analysis that will be undertaken in a future study. Large droplet sizes were sampled with the DMT CIP, which features 62 sizing bins with center sizes between 50 μm and 1600 μm (1.6 mm) and a width of 25 μm. Due to the more limited CIP sampling relative to other instruments (50 full profiles),

https://doi.org/10.5194/amt-2021-7
Preprint. Discussion started: 10 February 2021


Atmospheric Measurement Techniques Discussions

we only use CIP data to infer the precipitation contribution to the total in-situ cloud effective radius and how this could affect the analysis interpretation.

Flight level (~ 7 km ASL) solar reflectance measurements taken at 2.26 μm (0.865 μm) from the airborne NASA GISS RSP while above cloud were used to derive r_e (τ). Given the operational limitations of the CDP probe, RSP cloud products are a key dataset for this evaluation. The RSP features nine spectral bands between 410 nm and 2260 nm, with a field of view of 14 mrad, 14 mrad spacing between samples, and a scan swath of ± 60˚ relative to nadir. The RSP polarimetric r_e retrieval algorithm uses the polarized reflectance information contained in the backscattering angles ranging between 137˚ and 165˚ (*Alexandrov et al.*, 2012). The retrieval method exploits the fact that the polarized reflectance in the rainbow angular range is well-characterized by a unique combination of cloud effective radius and effective variance of the droplet size distribution. This justifies a parameterization that fits the angular shape of the polarized reflectance using an analytical equation dependent on scattering angle and scattering phase matrix, which in turn, is calculated via Mie theory from r_e and the effective variance of a gamma-size distribution (*Hansen and Travis*, 1974). A numerical assessment of the RSP using synthetic observations derived from a large-eddy simulation model quantifies an accuracy of RSP r_e generally better than 0.15 μm, with retrievals insensitive to three-dimensional radiative transfer effects (*Alexandrov et al.*, 2012). In addition, analysis of RSP r_e for NAAMES showed good quantitative agreement with CDP r_e within about 100 m of the cloud top (Alexandrov et al., 2018). Unlike r_e, τ from the RSP is derived using a standard reflectance-based method that finds a value for τ that yields the best match between the observed 864-nm nadir reflectance and its simulated counterpart estimated with a one-dimensional radiative transfer model, and constrained with the polarization-based r_e.

2.2.Satellite observations

The satellite cloud retrievals evaluated in this study are from GOES-13 and MODIS onboard Terra and Aqua. While GOES-13 observes the NAAMES domain continuously (GOES-13 is fixed relative to Earth, and located at 75˚W), Terra and Aqua daytime overpasses occur at approximately 10:30 and 13:30 local solar time (15:30 and 18:30 UTC), respectively. Cloud optical depth and effective radius are retrieved using CERES Edition 4 algorithms (*Minnis et al.*, 2011; 2020) applied to MODIS using the 0.64 μm and 3.79 μm channels. CERES adopted these channels for τ and r_e derivation because their radiometric equivalents are common to many other sun-synchronous and geostationary satellite imagers that are currently ingested by the CERES program. The CERES-MODIS algorithms have been adapted to utilize similar channel combinations on geostationary (*Minnis et al.*, 2008) and other lower Earth-orbiting satellites (*Minnis et al.*, 2011, 2016) and integrated into the NASA Satellite ClOud and Radiation Property System (SatCORPS) to produce historical and near-realtime datasets for use in research and operations. Here, the SatCORPS uses the GOES-13 0.65 and 3.90-μm channels, with the visible radiances being calibrated against Aqua-MODIS following *Doelling et al.* (2018).

The SatCORPS team at NASA Langley provided near-real time satellite support for the NAAMES operations (https://satcorps.larc.nasa.gov/NAAMES-2015). This support included GOES-13 images and SatCORPS cloud

https://doi.org/10.5194/amt-2021-7
Preprint. Discussion started: 10 February 2021


Atmospheric Measurement Techniques Discussions

retrievals every 30 minutes at a nadir resolution of 4 km (3.90-μm channel resolution and 0.63-μm channel subsampled to 4-km resolution). In practice, given the high GOES viewing zenith angles (~65˚) for the NAAMES domain, the actual resolution for the GOES-13 Imager is approximately 3.2 km x 9.3 km for the east-west and meridional components, respectively. To avoid retrievals with high uncertainties near twilight, we only use observations with solar zenith angles less than 75˚. During NAAMES 2017, GOES-13 and GOES-16 took coincident measurements over the NAAMES domain, with GOES-16 ultimately replacing GOES-13 when it was decommissioned in December 2017. Due to calibration uncertainties prior to official implementation in NOAA operations, GOES-16 is not evaluated against NAAMES observations. However, we inter-compare cloud products from the GOES-13 imager and the GOES-16 Advanced Baseline Imager (ABI) for December 2017 to provide a glimpse of improvements expected when using ABI data (Section 3.3.). In addition to an increased number of channels, ABI features better spatial resolution (2 km at nadir for 3.90 μm) relative to its GOES-13 predecessor (4 km).

The MODIS cloud products evaluated here are identical to the ones used to generate the CERES Single Scanner Footprint (SSF) product and are derived at the pixel resolution (1 km x 1 km at nadir and 4.8x2 km at the scan edge) for every other pixel due to computational constraints, to achieve an effective 2 km x 2 km resolution at nadir. Lastly, we note that the CERES cloud algorithms differ from those of the MODIS Science Team (Goddard Space Flight Center, *Platnick et al.*, 2017). Even though both products compare well with each other, especially for low-level liquid clouds, some differences should be expected. The reader is referred to *Painemal et al.* (2012), *Zhang et al.* (2018), and *Minnis et al.* (2020) for a more in-depth comparison between the CERES and MODIS Science Team products.

2.3. Matching method

Collocation of satellite data and the aircraft observations are performed separately for the airborne in-situ (CDP) and remotely-sensed (RSP) data collection, and depicted in Fig. 2.

2.3.1. Collocation with in-situ data: Prior to matching the in-situ and satellite data, we take into account that 3.79-3.9 μm satellite r_e is representative of the first few optical depths (~2) down from the cloud top (*Platnick*, 2000) where most of the absorption occurs for that band. Thus, this radiative signature implies that the r_e comparison needs to be performed with in-situ observations near the cloud top. For this purpose, we first estimate cloud boundaries (base and top) for continuous ascents and descent profiles by visually inspecting all the NAAMES in-cloud observations and use a minimum liquid water content threshold of 0.03 g m^{-3} to define a cloudy sample, a methodology that yields a total of 80 in-situ samples. Next, cloud-top r_e is computed for each profile by averaging r_e over the uppermost portion of the cloud above the $\tau = 2.0$ altitude level from the top. In the calculation of τ, we have assumed an extinction efficiency of 2.0, with cloud extinction coefficient estimated from the 2nd moment of the droplet size distribution, as in *Painemal and Zuidema* (2011). The r_e calculation is minimally sensitive to the τ threshold as variations of 1.0 and 3.0 yield changes in r_e close to 0.1 μm. Lastly, we match and average the closest 2x2 (GOES) and 4x4 (MODIS) pixels centered at the vertical profile location, with a temporal mismatch of less than 15 min for

https://doi.org/10.5194/amt-2021-7
Preprint. Discussion started: 10 February 2021


Atmospheric Measurement Techniques Discussions

GOES-13 and 25 min for MODIS. The 25 min window for MODIS reflects the limited number of satellite overpasses available and represents a compromise between obtaining a meaningful number of collocated samples and ensuring that the aircraft and MODIS are observing the same cloud features.

2.3.2. Collocation with RSP: The two primary advantages of airborne RSP retrievals, relative to in-cloud CDP observations, is the increased spatiotemporal sampling and the satellite-RSP consistency in the sense that RSP r_e is mostly sensitive to the cloud top (τ~1), similar to GOES and MODIS. Given the relatively narrow RSP field of view (~ 70 m for NAAMES, *Alexandrov et al.*, 2018), the RSP retrievals were averaged along the flight track to make it comparable to the satellite pixel resolution. Given an aircraft speed that ranges between 130-155 m/s during the high-altitude aircraft transects (when RSP sampled boundary layer clouds), we use a 134-s average window, equivalent to a horizontal scale of at least 16 km. From the central latitude and longitude of this window, a 16-km diameter allows for collocating around 2 north-south pixels for GOES-13 (4 subsampled pixels for MODIS) with the RSP retrievals, consistent with the methodology used for satellite-CDP collocation. As in the in-situ collocation, the aircraft-satellite temporal mismatch is less than 15 min and 25 min for the GOES imagers and MODIS, respectively. Consistency across the different analyses within this work indicates that the matching discrepancy between MODIS and GOES-13 has a negligible effect.

3. Results

3.1. Evaluations of satellite-derived cloud effective radius against CDP measurements

Before describing the main results, we first provide an overview of the cloud vertical structure during the campaign. The profiles in Fig. 3 are normalized by their maximum value, and cloud base and top are denoted, respectively, by 0 and 1 in the vertical coordinate (Z_N). Given the normalization applied to the data, uncertainties in the CDP should have a negligible impact in the result interpretation. The liquid water content profiles (Fig 3a), on average, linearly increase with height until it sharply decreases at the cloud top. Similarly, r_e linearly increases toward the cloud top, whereas N_d is relatively homogeneous with height. While the vertical variability is substantial, the mean cloud structure observed in NAAMES is similar to that observed in more archetypal subtropical stratocumulus clouds (e.g. *Painemal and Zuidema*, 2011). Two key aspects that emerge from the normalized profiles are: a) r_e is a maximum near the cloud top, and b) a vertically stratified cloud model is expected to fit the observations reasonably well, implying that liquid water path (LWP) can be more precisely estimated by $LWP = \frac{5}{9} \cdot \rho \cdot r_e \cdot \tau$ (with ρ denoting the liquid water density), as opposed to the vertically homogeneous equation $LWP = \frac{2}{3} \cdot \rho \cdot r_e \cdot \tau$, as suggested by studies in the subtropics (e.g., *Seethala and Horvath*, 2010; *Painemal et al.*, 2017).

Comparisons of satellite r_e against its in-situ counterpart (Fig. 4 and Table 1) reveal correlations of 0.68 for GOES and 0.58 for MODIS, with systematic positive biases. The overestimation by GOES reaches a value of 4.8 μm

https://doi.org/10.5194/amt-2021-7
Preprint. Discussion started: 10 February 2021


Atmospheric Measurement Techniques Discussions

(45.7%), which is more than twice that observed for MODIS (1.7 μm, 16.2%). Similarly, the root mean square error (RMSE) is higher for GOES-13 (5.8 μm) than MODIS (2.9 μm). These findings are confirmed in the next section with the use of RSP data.

3.2. Evaluations of satellite-derived cloud effective radius and optical depth against RSP retrievals

The RSP-satellite r_e linear correlation coefficient (r) is 0.52 for GOES and 0.68 for MODIS (Fig. 5). A persistent positive bias is also confirmed for both satellite sensors, with values of 5.3 μm (51.6%) for GOES, and 2.60 μm (25.8%) for MODIS, slightly greater than those estimated from the CDP probe. The effect of spatial inhomogeneity in satellite r_e was assessed by means of the τ coefficient of variation (χ), determined as the ratio of the standard deviation to the mean RSP cloud optical depth (similar to *Liang et al*, 2009). The most heterogeneous samples, defined as the top χ quintile (χ>0.8, Fig 5, filled blue circles) were contrasted against the rest of the samples. For GOES-13, comparing against heterogeneous samples (χ>0.8) yields a modest bias increase relative to samples with χ≤0.8 (5.8 and 5.2 μm, respectively). Yet, the effect of heterogeneity on satellite r_e are consistent with the overestimation that is expected for subpixel variability in cloud reflectances, although we note that the effects of heterogeneity are greatly ameliorated for r_e retrievals estimated from the 3.7-3.9 μm band relative to those based on shorter wavelengths (*Painemal et al.*, 2013).

We repeat the analysis above, but applied it to τ (Fig. 6). The satellite and RSP τ yield higher linear correlation coefficients than those for r_e, (r = 0.76), with the satellite underestimating airborne τ by -3.0 for both GOES-13 and MODIS. Unlike the r_e comparison, the effect of the scene heterogeneity in satellite τ is evident, with negative biases reaching, respectively, -10.9 and -8.2 for GOES and MODIS for highly heterogeneous fields (χ>0.8). In contrast, more homogenous samples (χ≤0.8) yield a reduced bias of -1.2 (GOES) and -1.7 (MODIS), which further decreases to -0.72 and -0.20 for scenes with χ<0.5.

3.3. GOES-13 and MODIS Inter-comparison

We further inter-compare both satellite products to gain insight into the discrepancies between GOES and MODIS manifested in their different r_e biases. We gridded the satellite data at 0.25˚ spatial resolution and matched them to within 15 min of the satellite overpasses for the NAAMES days over the oceanic domain bounded by 50˚W-35˚W, 40˚N-60˚N. The comparison for overcast grids shows that the GOES-13 r_e is larger than both Terra-MODIS (1.9 μm, Fig. 7a) and Aqua-MODIS (2.0 μm, Fig. 8a) and the linear correlations are r = 0.84-0.90. By contrast, GOES and MODIS τ values exhibit smaller differences (<0.7), a smaller mean GOES τ, and comparable correlations with r = 0.90 (Figs. 7b and 8b). Differences between the GOES and MODIS retrievals likely reflect a) the fixed viewing geometry of GOES with an average viewing zenith angle of 64˚, and b) higher MODIS pixel resolution. Both effects are illustrated in Fig. 9, in which the difference between GOES and MODIS (Terra and Aqua combined) cloud products

https://doi.org/10.5194/amt-2021-7
Preprint. Discussion started: 10 February 2021


Atmospheric Measurement Techniques Discussions

are binned as a function of MODIS viewing zenith angle (VZA). Differences in r_e decrease from nearly 2.2 μm near nadir to 1.5 μm close to the MODIS scan edge (~ 60˚, Fig 9a). τ differences also decrease with MODIS VZA (within 1.2), with negligible GOES-MODIS difference for grids collocated near the MODIS scan edge. Despite closer agreement between GOES-13 and MODIS r_e for high MODIS VZA, systematically larger GOES-13 r_e than MODIS points to other factors in explaining the systematic biases for GOES-13.

While some aspects of the viewing geometry and illumination effects on MODIS r_e and τ have been explored to some degree in a number of studies (e.g., *Marshak et al.*, 2006; *Kato et al.*, 2009; *Horvath et al.*, 2014), it remains largely unknown to what extent previous analyses are applicable to geostationary sensor geometry. We have previously shown the sensitivity of the MODIS-GOES difference to VZA, consistent with the effect of pixel coarsening, and the non-linearity of the reflectance–r_e and –τ relationship dependent on VZA (*Liang and DiGirolamo*, 2013). Another geometrical parameter of interest is the satellite scattering angle (Θ), or the angle between the solar and satellite viewing direction, as it provides information about the cloud side viewed by the satellite (shadow or illuminated). For the data analyzed here, the GOES-13 grids matched with Terra and Aqua produce GOES Θ averages of 132.3˚ and 150.4˚, respectively. That is, GOES Θ in the afternoon is more oriented toward the backscattering direction. To examine the possibility of a bias dependence on Θ, we bin the r_e difference between GOES-13 and MODIS (Aqua and Terra) as a function of Θ (Fig. 10). It is found that the differences increase toward the backscattering direction, particularly for angles higher than 143˚, with changes of around 1.0 μm between the highest and lowest Θ bins. A similar analysis applied to MODIS Θ is more challenging because the range of MODIS Θ variability is narrower than GOES, and VZA and Θ cannot be fully disentangled.

4. Discussion

Since the comparisons were made using the cloud mode of the CDP particle size distribution, the potential effects of precipitation unaccounted for in the calculations is addressed here. This is because satellite retrievals can be positively biased relative to cloud mode observations under the presence of a precipitation mode not considered in the Mie calculations (*Nakajima et al.,* 2010). The potential role of precipitation is indirectly assessed by comparing near-cloud-top CDP r_e (cloud mode) and that derived from the CDP and CIP droplet size distribution, after discarding the first bin of the CIP probe (52 μm) to remove instrument sizing overlap. We found that total r_e (CDP+CIP) is 0.41 μm larger than that from the CDP, a discrepancy that is much smaller than the difference between satellite and in-situ r_e. This result is somewhat expected as precipitation tends to be weighted toward the cloud base, becoming an unlikely cause for satellite-aircraft discrepancy. It is possible that this effect becomes more relevant for shorter wavelengths, characterized by a deeper photon penetration into the cloud (e.g. 1.6 μm channel; *Platnick*, 2000). However, determining the extent of the precipitation-driven bias for other satellite channels is difficult, as r_e estimated from shorter infrared wavelengths is more prone to subpixel variability and 3D radiative effects, which also yield particle size overestimations (e.g. *Zhang et al.*, 2012).

https://doi.org/10.5194/amt-2021-7
Preprint. Discussion started: 10 February 2021


Atmospheric Measurement Techniques Discussions

The effect of spatial resolution on the GOES-13 retrievals is explored by comparing GOES-13 and GOES-16 ABI for five days in December 2017, two months after the last NAAMES aircraft deployment. During December, both GOES satellites operated over the same region, implying nearly identical viewing geometries. With GOES-16 becoming the operational GOES-16, GOES-13 drifted to reach its final location at 60˚ E in January 2018. ABI pixel resolution is 2x2 km at nadir, and 2.8x4.6 km for the NAAMES region, whereas the resolution of the GOES-13 Imager is 3.1 x 9.3 km. GOES-16 and GOES-13 cloud products are retrieved with a very similar algorithm, with visible channels calibrated against Aqua-MODIS, and therefore, any inter-satellite discrepancy should be primarily attributed to the imagers' spatial resolution. Bivariate histograms of 0.25˚ averaged grids from GOES-16 and GOES-13 for the NAAMES domain are depicted in Fig. 11. GOES-13 r_e is well correlated with GOES-16 (r =0.97), with GOES-13 sizes 0.7 μm larger than GOES-16 (Fig. 11a). A similar analysis applied to τ produce comparable correlations (r= 0.93), with GOES-13 τ being 3.4 less than that for GOES-16 (Fig. 11b). The τ negative bias systematically increases with GOES-16 τ, with differences of -1.1 and -5.8 for GOES-16 τ of less than and more than 20, respectively. We note that December was characterized by optically thicker clouds than those observed during NAAMES, possibly attributed to the presence of low clouds driven by winter midlatitude weather disturbances. The observed intersatellite differences are consistent with the effect of subpixel variability and the non-linearity between reflectance and r_e and τ. As the pixel resolution is degraded, the convex (concave) shape of the reflectivity- r_e (τ) curve yields a retrieved r_e (τ) from the pixel reflectance that is larger (smaller) than the average r_e (τ) for that pixel. Larger negative biases in τ as τ increases also appear to be linked to the concavity relationship in which the non-linear τ-reflectivity relationship means that τ errors are accentuated for higher reflectances.

An additional factor known to severely affect plane-parallel cloud retrievals are 3D radiative transfer effects. While their influence is generally attenuated as the spatial averaging increases (pixel resolution coarsening, *Marshak et al.*, 2006), for a specific combination of viewing angle, illumination, and cloud morphology, satellite-derived optical properties can be severely biased. This issue has been partially addressed here by examining the dependence on satellite scattering angle, which is generally assumed to provide information regarding cloud shadowing for the forward scattering view (Θ<90), and enhanced illumination for the backscattering directions (Θ>90). Under this simple framework, it is generally interpreted that high values of reflectance at the backscattering direction are associated with an overestimation of τ and underestimation of r_e, and vice versa for the forward scattering direction where shadowing occurs (*Kato et al.*, 2006). Indeed, MODIS observations over Brazil have shown differences between forward and backscattering angles up to 6 μm for r_e for cumulus clouds (*Vant-Hull et al.*, 2007). Surprisingly, we found instead that GOES r_e increases in the backscattering direction, reaching a cloud effective radius at Θ ≥ 148˚ that is between 0.3 – 1.0 μm greater than that for Θ =116˚. This small r_e increase with Θ in the backscattering direction was also observed by *McHardy et al.* (2018) over the continental U.S. for GOES-East and West. Moreover, they found that the expected increase in r_e due to cloud shadowing (forward scattering) is only apparent for Θ <90˚, with an increase greater than 10 μm for Θ =60˚.

The positive bias in GOES-13 r_e for the backscattering direction is somewhat consistent with other studies that report modest MODIS r_e increase over specific oceanic regions (e.g. *Horvath et al.*, 2014; *Liang et al.*, 2015).

https://doi.org/10.5194/amt-2021-7
Preprint. Discussion started: 10 February 2021


Atmospheric Measurement Techniques Discussions

However, since Θ, latitudinal location, and viewing zenith angle are not decoupled in the MODIS data, isolating the effect of satellite scattering angle on MODIS retrievals is a challenge. Unlike MODIS, a wide range of scattering angles can be readily sampled by geostationary sensors. For instance *Arduini et al.* (2005) found for angles in the vicinity of the rainbow scattering angle (~140˚) a strong dependence of GOES r_e on the prescribed effective variance of the droplet size distribution, and a limited effect on τ. Building upon *Arduini et al.* (2005), *Benas et al.* (2019) retrieved τ and r_e from the Spinning Enhanced Visible and Infrared Imager (SEVIRI), onboard Meteosat-8 and 10, for a set of effective variances over the southeast Atlantic Ocean. They found that increasing the effective variance in the algorithm yields larger r_e near the rainbow and smaller r_e at the glory. Moreover, *Benas et al.* (2019) also noted that small effective variances tend to produce a more homogeneous diurnal cycle by reducing local discontinuities for the glory and rainbow angles. The exploratory analyses of *Arduini et al.* (2005) and *Benas et al.* (2019) leave, nevertheless, several unaddressed aspects such as the role of solar zenith angle, the contribution of 3D radiative effects, and the dependence of r_e on the effective variance for a broad r_e range. Currently, the CERES and SatCORPS cloud algorithms use a cloud model with a gamma-distribution effective variance of 0.1, which is higher than those observed over the ocean and less than those over land according to the literature review in *Benas et al.* (2019). For the nearly 80 profiles used in this study, we confirm that the effective variance is typically less than 0.1 (Fig. 11), with a mean value of 0.05 near the cloud top and 0.07 for the averaged cloud profiles. Future work will concentrate on deriving cloud retrievals based on Mie calculations estimated using various droplet size distribution shapes to scrutinize their effect on effective radius biases in the backscattering direction.

5. Concluding Remarks

Airborne observations of cloud microphysical/optical properties of North Atlantic boundary layer clouds during NAAMES provided a suitable dataset for assessing cloud retrievals from GOES-13 and Terra/Aqua MODIS. The airborne dataset consists of in-situ r_e derived from the DMT CDP cloud probe, and retrievals of τ and r_e from NASA GISS RSP measurements. The polarimetric r_e retrievals from the RSP are largely insensitive to 3D radiative effects. This study provides one of the first satellite evaluations in midlatitudes poleward of 40˚, where both warm and supercooled boundary layer clouds are a climatological feature. Our main findings are summarized as follows.

1. Comparisons between GOES-13 and MODIS r_e and τ against airborne observations show good correlations: $r \geq 0.52$ for r_e and $r \geq 0.76$ for τ. Both satellite sensors yield positive r_e biases relative to the airborne data. The GOES-13 bias exceeds that of MODIS by at least 1.9 μm. The positive MODIS r_e bias is similar, if not slightly higher than that observed over the subtropical Southeast Pacific in *Painemal and Zuidema* (2011). The GOES-13 and MODIS retrievals underestimate the RSP τ by 3.0, a difference primarily explained by sub-pixel heterogeneity, in which retrievals for pixels in spatially heterogeneous cloud fields are less than the expected mean τ for the same pixels. In contrast, spatial inhomogeneity effects have a modest effect on r_e, consistent with the weak sensitivity of the 3.79-3.9 μm band to spatial inhomogeneity (*Zhang and Platnick*, 2011).

https://doi.org/10.5194/amt-2021-7
Preprint. Discussion started: 10 February 2021


Atmospheric Measurement Techniques Discussions

2. Part of the large GOES-13 r_e bias is caused by the high viewing zenith angle (~60˚) and the associated pixel coarsening. This effect is clearly observed when comparing GOES with MODIS for varying MODIS VZA. r_e differences range from 2.2 μm for MODIS near-nadir view, to 1.5 μm for a MODIS VZA similar to GOES VZA over the NAAMES region (~60˚). However, the discrepancy between GOES-13 and MODIS r_e is not completely removed, and thus, the GOES bias with respect to NAAMES observations remains high.

3. Pixel resolution effects are evaluated by comparing GOES-13 with GOES-16 when both satellites were situated close to each other, before GOES-13 drifted to its 60˚W position. We find that GOES-13 r_e is 0.7 μm larger than that from GOES-16. This difference is associated with a pixel area that decreases from 29.3 km^2 (GOES-13) to 12.9 km^2 (GOES-16). It is concluded that GOES-16 should yield a better agreement with ground-truth data, yet the satellite r_e overestimation is not removed.

4. Exploratory analysis is intended to determine the impact of satellite scattering angle Θ on r_e. GOES-13 r_e increases with Θ up to 1.0 μm relative to MODIS. The result is counterintuitive as the backscattering direction is expected to be associated with r_e underestimation as the sensor views the bright side of the cloud. We lack a definitive explanation for the Θ- r_e relationship, and thus, future work will address this with the use of a larger satellite dataset. Lastly, although GOES biases attributed to backscattering direction, high VZA, and pixel resolution might not be exactly additive, their magnitudes could well explain the discrepancy between GOES and MODIS.

Our assessment confirm some results in *Ahn et al.* (2018), which was, to the best of our knowledge, the only MODIS assessment at high latitudes over the ocean based on in-situ aircraft. Southern Ocean clouds reported in *Ahn et al.* (2018) correspond to highly broken stratocumulus clouds, which pose challenging conditions for both airborne sampling and satellite remote sensing. Even though they found a positive bias in MODIS r_e (Goddard Space Flight Center Product Level 2) for non-precipitating clouds, their limited dataset prevented an in-depth analysis of the reasons for the overestimation. In addition, our findings are consistent with studies over the eastern Pacific, in which, MODIS and GOES retrievals correlate well with airborne data, with larger satellite r_e relative to in-situ r_e. While accounting for precipitation in the in-situ observation would decrease the MODIS r_e bias by 0.41 μm, the remaining discrepancy is possibly explained by a combination of viewing geometry and 3D radiative transfer effects (*Kato et al.*, 2006)

While independent aircraft datasets corroborated the results for satellite r_e, assessment of τ was based only on comparisons with the RSP τ, with no direct estimates of liquid water path (LWP). However, an indirect LWP comparison can be achieved by applying the relationship $LWP = \frac{5}{9} \cdot \rho \cdot r_e \cdot \tau$ to both RSP and satellite data (Section 3.1). The correlations between satellite and RSP LWP are high (r=0.67 for GOES-13 and r=0.73 for MODIS), with GOES-13 and MODIS LWP overestimating that from RSP by 17.0 g/m^2 and 9.5 g/m^2, for GOES-13 and MODIS, respectively. The satellite overestimation is caused by the r_e bias, which also explains the higher GOES-13 LWP bias compared to that for MODIS LWP.

Our analysis underscores less understood uncertainties in cloud retrievals from geostationary satellites caused by the fixed geometry and the broad range of viewing zenith and scattering angles not observed in MODIS. Future work will expand the analysis with a more comprehensive satellite dataset including inter-comparisons between GOES-

13/16 and Aqua/Terra as well as from other sun-synchronous satellites. Further, radiative simulations and the development of a geostationary simulator will be valuable for interpreting the observational relationships.

Data availability. NAAMES website is at https://naames.larc.nasa.gov. NAAMES data are publicly available at http://doi.org/10.5067/Suborbital/NAAMES/DATA001 (last access: July 19, 2019). GOES-13 cloud retrievals are available at: https://satcorps.larc.nasa.gov/NAAMES-2015 (last access: March 20, 2020) and the latest data for flight days are also available upon request.

Author contributions. DP designed the study, and DP and DS carried out the analysis. DP prepared the manuscript with contributions from all the co-authors. PM and WS helped with the interpretation of the satellite analysis, BC, EC, and RM provided their insight on the use of NAAMES in-situ and remotely sensed observations. BC, RM, EC, CR, KT, EW, and LZ collected the airborne in-situ and remotely sensed observational data during NAAMES.

Competing interests. The authors declare that they have no conflict of interest.

Financial support. This work was funded by the NAAMES project and the CERES program. RM was partially supported by a NASA New Investigator (Early Career) Program award.

Acknowledgements: We thank the NAAMES aircraft Team and PI Dr. Michael Behrenfeld for their tireless efforts during the 5-year project. GOES processing by Rabindra Palikonda is greatly appreciated.

References

Ahn, E., Y. Huang, S. T. Siems, and M. J. Manton (2018), A comparison of cloud microphysical properties derived from MODIS and CALIPSO with in situ measurements over the wintertime Southern Ocean, *J. Geophys. Res.: Atmos.*, *123*, 11,120– 11,140, doi:10.1029/2018JD028535.

Alexandrov, M. D., B. Cairns, C. Emde, A. S. Ackerman, and B. van Diedenhoven (2012), Accuracy assessments of cloud droplet size retrievals from polarized reflectance measurements by the research scanning polarimeter, *Remote Sens. Environ.*, *125*, 92-111, doi:10.1016/j.rse.2012.07.012.

Alexandrov, M.D., et al. (2018), Retrievals of cloud droplet size from the research scanning polarimeter data: Validation using in situ measurements, *Remote Sens. Environ.*, *210*, 76-95, doi:10.1016/j.rse.2018.03.005

Arduini, R. F., P. Minnis, and J. K. Ayers, 2005: Sensitivity of satellite-derived cloud properties to the effective variance of cloud droplet size distribution. *Proc. 15th ARM Sci. Team Mtg.,* Daytona Beach, FL, March 14-18. (Available at http://www.arm.gov/publications/proceedings/conf15/extended_abs/arduini_rf.pdf)

Behrenfeld, M. et al. (2019), The North Atlantic Aerosol and Marine Ecosystem Study (NAAMES): Science motive and mission overview, *Frontiers in Marine Science*, *6*:122. doi: 10.3389/fmars.2019.00122.

https://doi.org/10.5194/amt-2021-7
Preprint. Discussion started: 10 February 2021

Benas, N., J. F. Meirnik, M. Stengel, and P. Stamnes (2019), Sensitivity of liquid cloud optical thickness and effective radius retrievals to cloud bow and gloary conditions using two SEVIRI imagers, *Atmos. Meas. Tech.*, *12*, 2863-2879, doi:10.5194/amt-12-2863-2019.

Benjamin, S. G., et al. (2016), A North American hourly assimilation and model forecast cycle: The Rapid Refresh, *Mon. Wea. Rev.* 144, 1669-1694. doi:10.1175/MWR-D-15-0242.1.

Doelling, D., C. Haney, R. Bhatt, B. Scarino, and A. Gopalan (2018), Geostationary visible imager calibration for the CERES SYN1deg Edition 4 Product, *Remote Sens. 10*, 288.

Hansen, J.E., L.D. Travis (1974), Light scattering in planetary atmospheres. *Space Sci. Rev.* **16**, 527–610.

Horváth, Á., C. Seethala, C., and H. Deneke (2014), View angle dependence of MODIS liquid water path retrievals in warm oceanic clouds, *J. Geophys. Res. Atmos.*, *119*, 8304– 8328, doi:10.1002/2013JD021355.

Hu, Y., S. Rodier, K. Xu, W. Sun, J., Huang, B. Lin, P. Zhai, P., and D. Josset, (2010), Occurrence, liquid water content, and fraction of supercooled water clouds from combined CALIOP/IIR/MODIS measurements, *J. Geophys. Res.*, *115*, D00H34, doi:10.1029/2009JD012384.

Jones, T. A., P. Skinner, K. Knopfmeier, E. Mansell, P. Minnis, R. Palikonda, and W. L. Smith, Jr. (2018), Comparison of cloud microphysics schemes in a Warn-on-Forecast system using synthetic satellite objects, *Wea. Forecasting*, *33*, 1681-1708, doi:10.1175/WAF-D-18-0112.1

Kato, S., L. M. Hinkelman, and A. Cheng (2006), Estimate of satellite-derived cloud optical thickness and effective radius errors and their effect on computed domain-averaged irradiances, *J. Geophys. Res.*, *111*, D17201, doi:10.1029/2005JD006668.

Kato, S., et al. (2011), Improvements of top-of-atmosphere and surface irradiance computations with CALIPSO-, CloudSat-, and MODIS-derived cloud and aerosol properties, *J. Geophys. Res.*, *116*, D19209, doi:10.1029/2011JD016050.

Liang, L., L. Di Girolamo, and S. Platnick (2009), View-angle consistency in reflectance, optical thickness and spherical albedo of marine water-clouds over the northeastern Pacific through MISR-MODIS fusion, *Geophys. Res. Lett.*, *36*, L09811, doi:10.1029/2008GL037124.

Liang, L., and L. Di Girolamo (2013), A global analysis on the view-angle dependence of plane-parallel oceanic liquid water cloud optical thickness using data synergy from MISR and MODIS, *J. Geophys. Res. Atmos.*, *118*, 2389– 2403, doi:10.1029/2012JD018201.

Liang, L., Di Girolamo, L., and Sun, W. (2015), Bias in MODIS cloud drop effective radius for oceanic water clouds as deduced from optical thickness variability across scattering angles. *J. Geophys. Res. Atmos.*, 120, 7661– 7681.

Loeb, N. G., et al. (2009), Toward optimal closure of the Earth's top-of-atmosphere radiation budget, *J. Clim.*, *22*, 748–766.

Marshak, A., S. Platnick, T. Várnai, G. Wen, and R. F. Cahalan, (2006), Impact of three-dimensional radiative effects on satellite retrievals of cloud droplet sizes, *J. Geophys. Res.*, *111*, D09207, doi:10.1029/2005JD006686.

https://doi.org/10.5194/amt-2021-7
Preprint. Discussion started: 10 February 2021

McHardy, T. M., X. Dong, B. Xi, M. M. Thieman, P. Minnis, and R. Palikonda (2018), Comparison of daytime low-level cloud properties derived from GOES and ARM SGP measurements, *J. Geophys. Res.*, *123*, 8221-8237, doi: 10.1002/2018JD0228911.

Minnis, P., et al. (2008), Near-real time cloud retrievals from operational and research meteorological satellites, In *Proc. SPIE Remote Sens. Clouds Atmos. XIII,* Cardiff, Wales, UK, 15–18 September, pp. 710703-710703-8, https://doi.org/ 10.1117/12.800344.

Minnis, P., et al. (2008), Cloud detection in non-polar regions for CERES using TRMM VIRS and Terra and Aqua MODIS data. *IEEE Trans. Geosci. Remote Sens.*, *46*(*11*), 3857– 3884.

Minnis, P., et al. (2011). CERES Edition-2 cloud property retrievals using TRMM VIRS and Terra and Aqua MODIS data, part I: Algorithms. *IEEE Trans. Geosci. Remote Sens.*, *49*(*11*), 4374– 4400.

Minnis, P., K. Bedka, Q. Trepte, C. R. Yost, S. T. Bedka, B. Scarino, K. Khlopenkov, and M. M. Khaiyer (2016), A consistent long-term cloud and clear-sky radiation property dataset from the Advanced Very High Resolution Radiometer (AVHRR). *Climate Algorithm Theoretical Basis Document (C-ATBD)*, *CDRP-ATBD-0826 AVHRR Cloud Properties - NASA*, NOAA CDR Program, 19 September, 159 pp., DOI:10.7289/V5HT2M8T. Available at https://www1.ncdc.noaa.gov/pub/data/sds/cdr/CDRs/AVHRR_Cloud_Properties_NASA/AlgorithmDescription_01B-30b.pdf

Minnis, P., et al. (2020). CERES MODIS cloud product retrievals for Edition 4, Part I: Algorithm changes, *IEEE Trans. Geosci. Remote Sens.*, *58*, doi:10.1109/TGRS.2020.3008866.

Nakajima, T. Y., K. Suzuki, and G.L. Stephens (2010), Droplet growth in warm water clouds observed by the A-Train. Part I: Sensitivity analysis of the MODIS-derived cloud droplet sizes, *J. Atmos. Sci., 67*, 1884–1896, https://doi.org/10.1175/2009JAS3280.1

Noble, S. R., and Hudson, J. G. (2015), MODIS comparisons with northeastern Pacific in situ stratocumulus microphysics, *J. Geophys. Res. Atmos.*, 120, 8332– 8344, doi:10.1002/2014JD022785.

Painemal, D., and P. Zuidema (2011), Assessment of MODIS cloud effective radius and optical thickness retrievals over the Southeast Pacific with VOCALS-REx in situ measurements, *J. Geophys. Res.*, *116*, D24206, doi:10.1029/2011JD016155.

Painemal, D., P. Minnis, J. K. Ayers, and L. O'Neill (2012), GOES-10 microphysical retrievals in marine warm clouds: Multi-instrument validation and daytime cycle over the southeast Pacific, *J. Geophys. Res.*, *117*, D19212, doi:10.1029/2012JD017822.

Painemal, D., P. Minnis, and S. Sun-Mack (2013), The impact of horizontal heterogeneities, cloud fraction, and liquid water path on warm cloud effective radii from CERES-like Aqua MODIS retrievals, *Atmos. Chem. Phys.*, *13*, 9997– 10,003, doi:10.5194/acp-13-9997-2013.

Painemal, D., C. Chiu, P. Minnis, M. Cadeddu, C. Yost, X. Zhou, E. Eloranta, E. Lewis, R. Ferrare, and P. Kollias (2017), Aerosol and cloud microphysics covariability in the northeast Pacific boundary layer estimated with ship-based and satellite remote sensing observations, *J. Geophys. Res. Atmos.*, *122*, 2403– 2418, doi:10.1002/2016JD025771.

https://doi.org/10.5194/amt-2021-7
Preprint. Discussion started: 10 February 2021

Platnick, S. (2000), Vertical photon transport in cloud remote sensing problems, *J. Geophys. Res.*, *105*, 22,919– 22,935, doi:10.1029/2000JD900333.

Platnick *et al*. (2017), The MODIS cloud optical and microphysical products: Collection 6 updates and examples from Terra and Aqua, *IEEE Trans. Geosci. Remote Sens.*, *55*, 502-525.

Roebeling, R., B. Baum, R. Bennartz, U. Hamann, A. Heidinger, J.F. Meirink, M. Stengel, A. Thoss, A. Walther, and P. Watts (2015), Summary of the Fourth Cloud Retrieval Evaluation Workshop, *Bull. Amer. Meteor. Soc., 96*, ES71–ES74, https://doi.org/10.1175/BAMS-D-14-00184.1

Seethala, C. and Á. Horváth (2010), Global assessment of AMSR-E and MODIS cloud liquid water path retrievals in warm oceanic clouds, *J. Geophys. Res.*, *115*, D13202, doi:10.1029/2009JD012662.

Stubenrauch, C.J., W. B. Rossow, S. Kinne, S. Ackerman, G. Cesana, H. Chepfer, B. Getzewich, L. DiGirolamo, A. Guignard, A. Heidinger, B. Maddux, P. Menzel, P. Minnis, C. Pearl, S. Platnick, C. Poulsen, J. Riedi, S. Sun-Mack, A. Walther, D. Winker, S. Zeng, and G. Zhao (2013), Assessment of global cloud datasets from satellites: Project and database initiated by the GEWEX Radiation Panel, *Bull. Amer. Meteor. Soc., 94*, 1031–1049

Trepte Q. Z. *et al*. (2019), Global cloud detection for CERES Edition 4 using Terra and Aqua MODIS data, *IEEE Trans. Geosci. Remote Sens.*, *57*, 9410-9449, doi:10.1109/TGRS.2019.2926620.

Vant-Hull, B. A. Marshak, L. A. Remer, and Z. Li (2007), The effects of scattering angle and cumulus cloud geometry on satellite retrievals of cloud droplet effective radius, *IEEE Trans. Geosci. Remote Sens.*, *45*, doi:10.1109/TGRS.2006.890416.

Zhang, Z., Ackerman, A. S., Feingold, G., Platnick, S., Pincus, R., and Xue, H. (2012), Effects of cloud horizontal inhomogeneity and drizzle on remote sensing of cloud droplet effective radius: Case studies based on large-eddy simulations, *J. Geophys. Res.*, 117, D19208, doi:10.1029/2012JD017655.

Zhang, Z., X. Dong, B. Xi, H. Song, P.-L. Ma, S. J. Ghan, S. Platnick, and P. Minnis (2017), Intercomparisons of marine boundary layer cloud properties from the ARM CAP-MBL campaign and two MODIS cloud products, *J. Geophys. Res. Atmos.*, *122*, 2351– 2365, doi:10.1002/2016JD025763.

https://doi.org/10.5194/amt-2021-7
Preprint. Discussion started: 10 February 2021

Atmospheric Measurement Techniques Discussions

Table 1: General r_e statistics between satellite and CDP probe observations. Percentage values are relative to mean CDP values matched with the satellite data.

	GOES-13 vs CDP			MODIS vs CDP		
	Bias	*r*	RMSE	Bias	*r*	RMSE
r_e	4.8 µm (45.7%)	0.68	5.8 µm (55.3%)	1.7 µm (16.2%)	0.58	2.9 µm (27.7%)

Table 2: General r_e and τ statistics between satellite and RSP retrievals. Percentage values are relative to mean RSP values matched with the satellite data.

	GOES-13 vs RSP			MODIS vs RSP		
	Bias	*r*	RMSE	Bias	*r*	RMSE
r_e	5.3 µm (51.6%)	0.52	6.6 µm (64.3%)	2.6 µm (25.8%)	0.68	3.6 µm (35.7%)
τ	-3.0 (-20.8%)	0.76	8.4 (58.3%)	-3.0 (20.3%)	0.77	7.4 (50.1%)

https://doi.org/10.5194/amt-2021-7
Preprint. Discussion started: 10 February 2021

Atmospheric Measurement Techniques Discussions

545

550

555

Figures

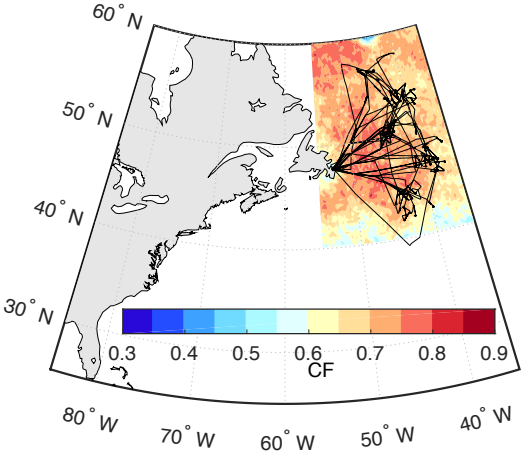

560 Figure 1: Mean Aqua-MODIS cloud cover during during the three campaigns in November 2015, May 2016, and September 2017 and aircraft tracks (black lines).

https://doi.org/10.5194/amt-2021-7
Preprint. Discussion started: 10 February 2021

Atmospheric Measurement Techniques Discussions

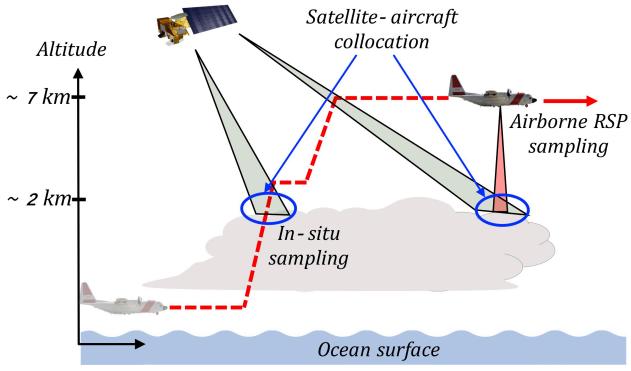

565 Figure 2: Collocation method between satellite and airborne in-situ (CDP probe) and RSP observations. Satellite pixels are paired with in-situ samples collected during profiling maneuver, whereas satellite and RPS data are collocated for high altitude aircraft transects (~ 7 km)

570

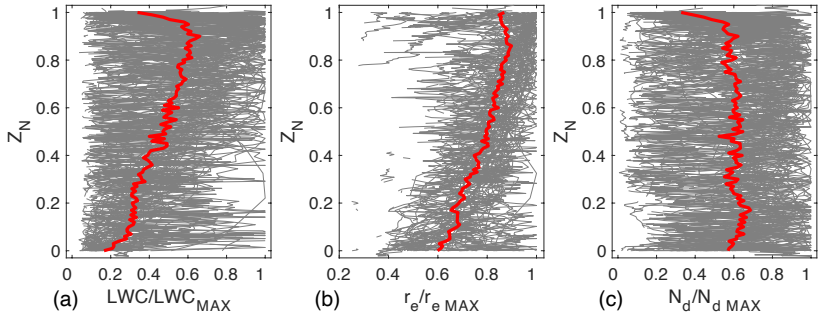

Figure 3: CDP profiles normalized by their maximum value: a) of liquid water content, (b), r_e, and c) cloud droplet number concentration N_dx. Normalized height (Z_N) corresponds to 0.0 for cloud base and 1.0 for cloud top height. Individual and mean profiles are depicted in gray and red, respectively.

575

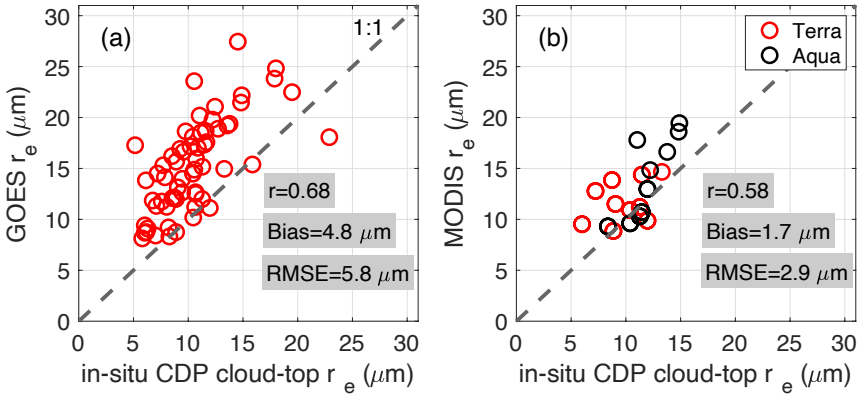

https://doi.org/10.5194/amt-2021-7
Preprint. Discussion started: 10 February 2021

Atmospheric Measurement Techniques Discussions

Figure 4: In-situ CDP cloud-top effective radius against a) GOES-13 and b) MODIS. Linear correlation coefficient is denoted by r, bias is calculated relative to the in-situ r_e, and RMSE is the root mean square error. Statistics for MODIS combine data from Aqua and Terra . Dashed line represents the 1-to-1 relationship.

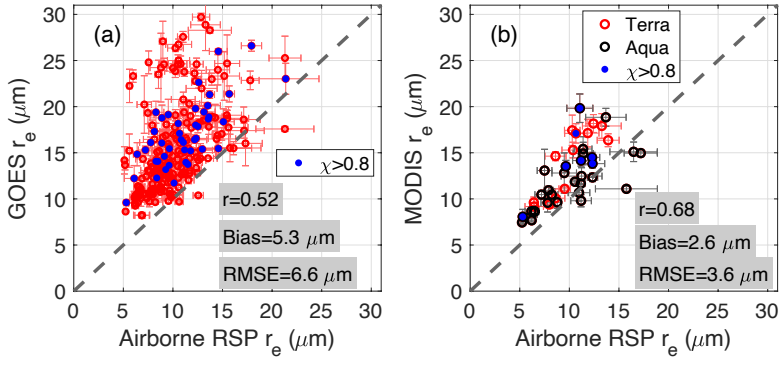

Figure 5: Relationship between airborne RSP r_e and (a) GOES-13 and (b) MODIS. Statistics for MODIS combine data from Aqua and Terra. Error bars denote the spatial standard deviation. Blue circles denote retrievals derived over highly heterogeneous cloud scenes.

https://doi.org/10.5194/amt-2021-7
Preprint. Discussion started: 10 February 2021

Atmospheric Measurement Techniques Discussions

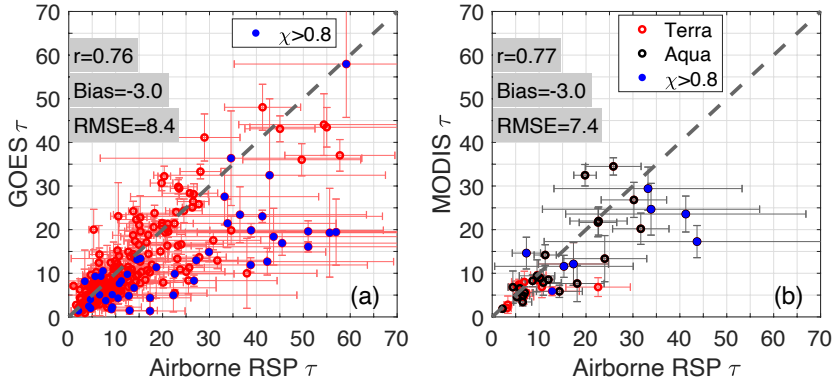

605 Figure 6: As Figure 5, but for the comparison between airborne RSP τ and (a) GOES-13 and (b) MODIS.

610

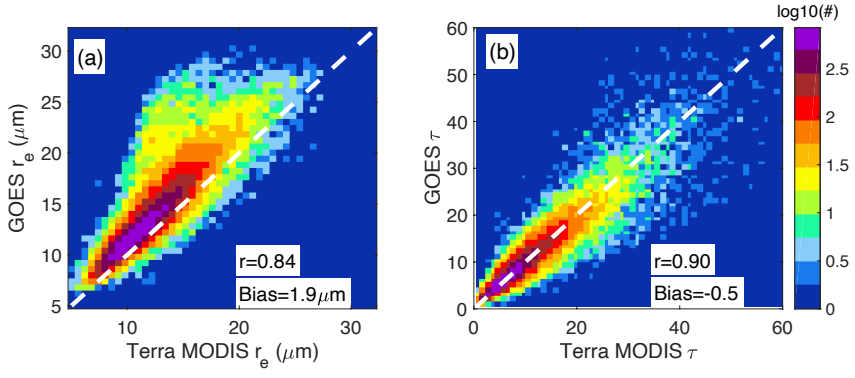

615 Figure 7: Bivariate histogram between Terra MODIS and GOES-13 a) r_e and b) τ. 1-to-1 line is denoted by the white dashed lines. Bias represents the mean difference between GOES-13 and MODIS.

https://doi.org/10.5194/amt-2021-7
Preprint. Discussion started: 10 February 2021

Atmospheric Measurement Techniques Discussions

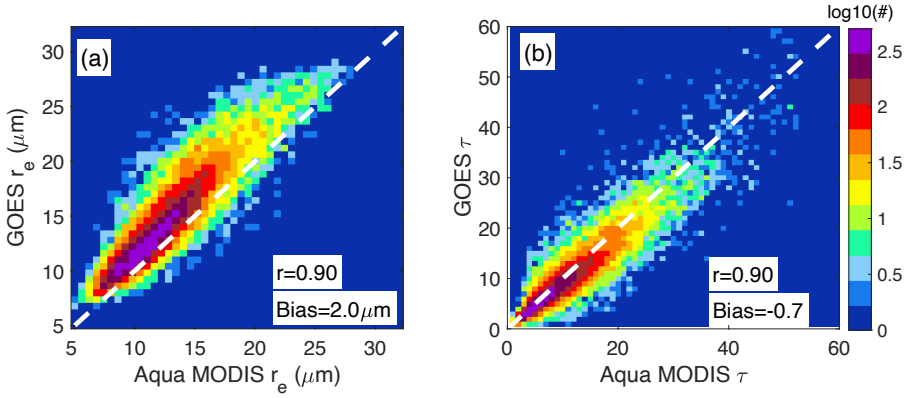

Figure 8: As Fig. 7 but for GOES-13 and Aqua-MODIS.

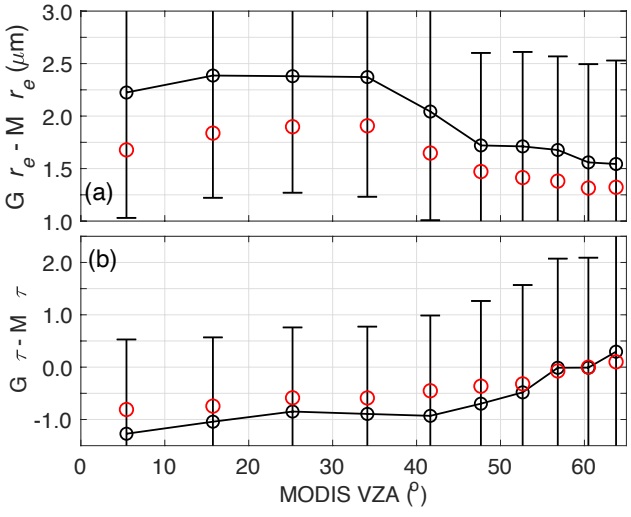

Figure 9: Mean differences between GOES and Aqua/Terra MODIS retrievals binned in MODIS VZA deciles: a) cloud effective radius, and b) cloud optical depth. Error bars denote the standard deviation, and median values are represented by red circles.

https://doi.org/10.5194/amt-2021-7
Preprint. Discussion started: 10 February 2021

Atmospheric Measurement Techniques Discussions

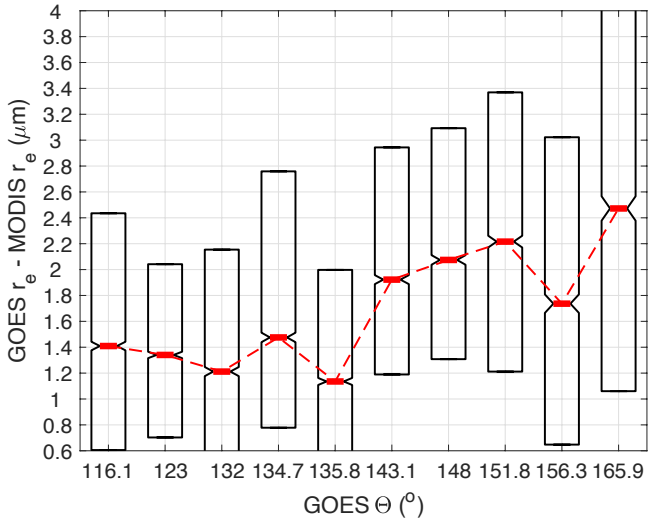

Figure 10: r_e differences between GOES-13 and MODIS (Aqua and Terra) binned in deciles of GOES-13 scattering angle (Θ). Middle horizontal lines in the box plot represent the median, lower and upper quartiles are indicated by the box boundaries. Notches are the 95% confidence interval of the median.

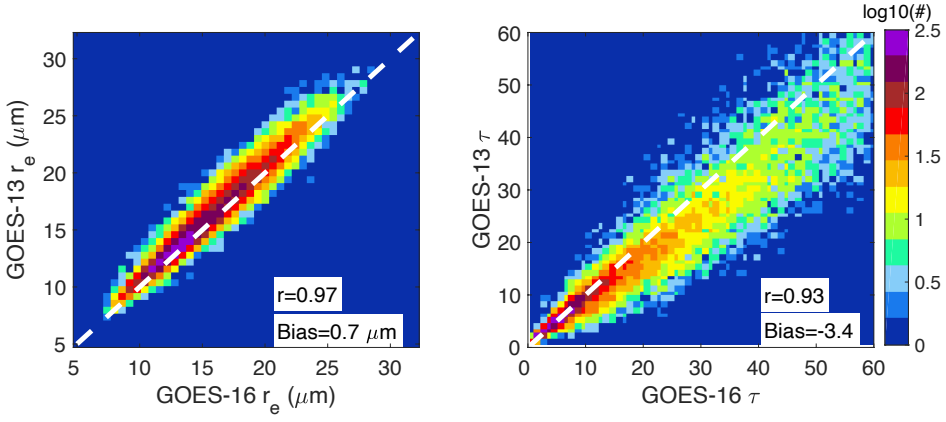

Figure 11: Relationship between 30-min GOES-16 ABI and GOES-13 cloud retrievals for 5 days of December 2017 (20, 22, 24, 26, 28) over the North Atlantic for solar zenith angle <75°: a) cloud effective radius and b) cloud optical depth. The bias is defined as the mean difference beween GOES-13 and GOES-16 retrievals.

https://doi.org/10.5194/amt-2021-7
Preprint. Discussion started: 10 February 2021

Atmospheric Measurement Techniques Discussions

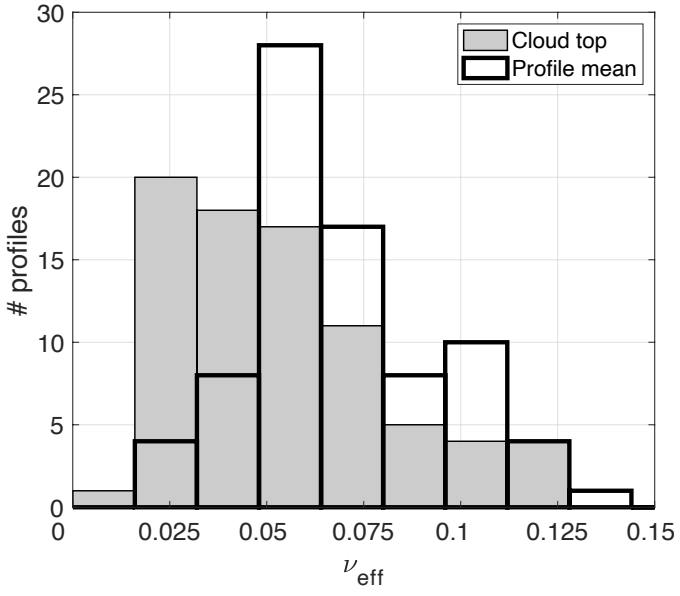

Figure 12: Histogram of computed effective variance (ν_{eff}) assuming a modified gamma distribution, for CDP values sampled near the cloud top (filled gray) and averaged throughout the cloud profile (black).

655